Journal Pre-proof

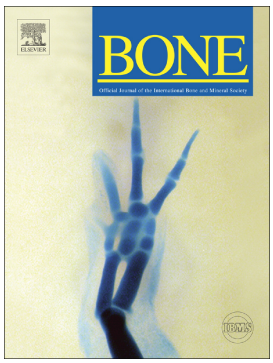


# A new ex vivo model of the bone tissue response to the hyperglycemic environment – The embryonic chicken femur organotypic culture in high glucose conditions

Rita Araújo, Victor Martin, Rita Ferreira, Maria Helena Fernandes, Pedro Sousa Gomes

PII: S8756-3282(22)00031-X

DOI: https://doi.org/10.1016/j.bone.2022.116355

Reference: BON 116355

To appear in: *Bone*

Received date: 28 December 2021

Revised date: 1 February 2022

Accepted date: 7 February 2022

Please cite this article as: R. Araújo, V. Martin, R. Ferreira, et al., A new ex vivo model of the bone tissue response to the hyperglycemic environment – The embryonic chicken femur organotypic culture in high glucose conditions, *Bone* (2021), https://doi.org/10.1016/j.bone.2022.116355

# A new ex vivo model of the bone tissue response to the hyperglycemic environment – the embryonic chicken femur organotypic culture in high glucose conditions

Rita Araújo[a,b] , Victor Martin[a,b], Rita Ferreira[c,d], Maria Helena Fernandes[a,b], Pedro Sousa Gomes[a,b]

a - Laboratory for Bone Metabolism and Regeneration, Faculty of Dental Medicine, University of Porto, Porto, Portugal
b - REQUIMTE/LAQV, University of Porto, Porto, Portugal
c - Department of Chemistry, University of Aveiro, Portugal.
d - REQUIMTE/LAQV, University of Aveiro, Aveiro, Portugal

Corresponding author:
Pedro de Sousa Gomes
Laboratory for Bone Metabolism and Regeneration - Faculty of Dental Medicine, University of Porto
Rua Dr. Manuel Pereira da Silva, 4220-393, Porto, Portugal
+351 220 901 100
pgomes@fmd.up.pt

Declarations of interest: none

**Abstract**

Diabetes mellitus (DM) embrace a group of chronic metabolic conditions with a high morbidity, causing deleterious effects in different tissues and organs, including bone. Hyperglycemia seems to be one of the most contributing etiological factors of bone-related alterations, altering metabolic functionality and inducing morphological adaptations. Despite the established models for the assessment of bone functionality in hyperglycemic conditions, in vitro studies present a limited representativeness given the imperfect cell-cell and cell-matrix interactions, and restricted three-dimensional spatial arrangement; while in vivo studies raise ethical issues and offer limited mechanistic characterization, given the modulatory influence of many systemic factors and/or regulatory systems.

Accordingly, the aim of this study is to establish and characterize an innovative *ex vivo* model of the bone tissue response to hyperglycemia, reaching hand of the organotypic culture of embryonic chicken femurs in high glucose conditions, showcasing the integrative responsiveness of the model regarding hyperglycemia-induced alterations. A thorough assessment of the cellular and tissue functionality was further conducted.

Results show that, in high glucose conditions, femurs presented an increased cell proliferation and enhanced collagen production, despite the altered protein synthesis, substantiated by the increased carbonyl content. Gene expression analysis evidenced that high glucose levels induced the expression of pro-inflammatory and early osteogenic markers, further impairing the expression of late osteogenic markers. Furthermore, the tissue morphological organization and matrix mineralization were significantly altered by high glucose levels, as evidenced by histological, histochemical and microtomographic evaluations.

Attained data is coherent with acknowledged hyperglycemia-induced bone tissue alterations, validating the models' effectiveness, and evidencing its integrative responsiveness regarding cell proliferation, gene and protein expression, and tissue morpho-functional organization. The assessed *ex vivo* model conjoins the capability to access both cellular and tissue outcomes in the absence of a systemic modulatory influence, outreaching the functionality of current experimental *in vitro* and *in vivo* models of the diabetic bone condition.

**Keywords**

Diabetes mellitus, hyperglycemic condition, bone tissue, bone metabolism, embryonic chicken femur, *ex vivo*.

## 1. Introduction

Diabetes mellitus (DM) embraces a group of chronic metabolic conditions that affects more than 400 million people worldwide, with an increasing prevalence, being estimated to affect over 600 million adults in 2045 [1]. It is associated with a high morbidity since it causes deleterious effects in different tissues and organs such as the heart, kidneys, nerves and blood vessels, with pathological mechanisms differing accordingly to its type [2]. Diabetes mellitus type 1 (T1DM) has commonly an early onset and it is caused by an autoimmune process that leads to destruction of pancreatic ß cells with subsequent insufficient insulin production. Insulinopenia and low levels of insulin-like growth factor-I (IGF-I) are characteristic of T1DM, alongside with poor glycemic control [3]. Diabetes mellitus type 2 (T2DM) has frequently a later onset and is caused by an increasing peripheral resistance to insulin, initially compensated by an increased insulin secretion to maintain glucose homeostasis that progressively fails with the disease progression, leading to hyperglycemia – a major contributor to its varied deleterious effects [2-4].

Regarding the relation of diabetes with bone tissue, literature presents some evidence of alterations regarding metabolic functionality and morphological adaptations. Studies show that T1DM patients present high fracture risk and low bone mineral density (BMD), while T2DM patients, despite regular or increased BMD, also report an increased fracture risk, possibly associated with bone microarchitectural changes [5-9]. Despite that hyperglycemia seems to be one of the most contributing factors to bone-related DM-related pathological effects - as addressed from in vivo [10-12] and clinical studies [13-17] - the underlying mechanisms are not fully understood [13], with major evidence arising from *in vitro* studies within bone cell populations [18-20].

Osteoblasts are bone forming cells that differentiate from mesenchymal stem cells (MSCs), which are primarily responsible for the secretion of the extracellular matrix (ECM) further mediating its mineralization [21, 22]. Some studies describe that hyperglycemia seems to impair osteoblastic activity by triggering cell apoptosis, due to the accumulation of advanced glycation products (AGE´s) [23, 24]. Other authors refer that hyperglycemia elevates the levels of some inflammatory mediators, such as interleukin-6 (IL-6) and tumor necrosis alpha factor (TNF-α) that may also trigger cell apoptosis [25]. Additionally, low levels of IGF-I may further impair osteoblastic differentiation, being an important inducer of osteogenesis [26]. Another aspect that seems to have an impact in bone development is the effect of hyperglycemia on MSC differentiation potential, as these cells have the ability to differentiate not only into the osteogenic lineage, but also into the chondrogenic or adipogenic pathways, among other mesenchymal lineages. MSCs differentiation is determined by microenvironmental biochemical stimuli such as hormones, cytokines, and other autocrine and paracrine factors, which leads to a defined lineage commitment. Some studies suggest that high glucose levels can divert differentiation of MSCs into adipocytes, even in the bone microenvironment, thus further impairing osteogenesis [27, 28]. Despite the verified hyperglycemia-related hindrances, *in vitro* studies offer limited cell-cell and cell-matrix interactions, and the restricted three-dimensional

spatial arrangement can lead to the loss of morpho-functional features of the cells, limiting data extrapolation [29, 30].

Within *in vivo* studies, osteopenia seems to be the major skeleton-related alteration associated with hyperglycemic conditions [5, 31-33]. Nonetheless, mechanistic studies are difficult to implement, given the influence of many systemic factors and/or regulatory systems modulating glucose bone metabolism. Experiments with animals are also expensive and often require the use of a large number of animals to obtain valid results, raising ethical questions [29, 30].

*Ex vivo* models have tried to close the gap between *in vitro* and *in vivo* models. These models conserve the three-dimensional arrangement of cells and ECM, as verified *in vivo*. Culture conditions are easier to manipulate in order to replicate physiological or pathological conditions, thus tissue responses can be evaluated without the influence of the diverse interacting systemic factors/regulatory systems [29, 30]. Literature describes several *ex vivo* models of bone tissue, used for various purposes such as the assessment of biomaterials and drugs, preclinical evaluation of therapeutic strategies and biomechanical assays. Besides, *ex vivo* models help to refine *in vivo* experiments, potentially reducing the number of used animals and minoring ethical issues [29, 30].

The embryonic chicken femur organotypic culture model has been used over the years, being well established in bone-related research [34-36]. It has been used for the evaluation of bone repair and testing of potential regenerative therapeutic approaches, as well as for the assessment of the bone biological response under distinct pathological conditions, with translational relevance to human applications [34]. Chicken embryos have a short-term development, are easy to manipulate, on their early stage of development are deprived of immune response and present a bone development process similar to the one verified in mammals. Those factors are the main contributors to its widespread use in relevant bone tissue-related research [34-37].

In this frame, and to the best of the authors' knowledge, the establishment and characterization of an *ex vivo* model of the bone response to hyperglycemic conditions has not been previously addressed. Thus, the present study aims to characterize the impact of high glucose in the embryonic chicken femur organotypic culture model, validating the establishment of a representative *ex vivo* system for the modulation of the hyperglycemic-related complications of the bone tissue, further evidencing the model's integrative responsiveness at the cellular and tissue levels.

## 2. Materials and methods

### 2.1 Embryonic chicken femora organotypic culture

Fertilized chick eggs (*Gallus domesticus*) were acquired from a local certified vendor. At day 11 of development embryos were euthanized and femora carefully dissected and cleaned, preserving the periosteum. Femora were then transferred to Netwel™ inserts (440 µm mesh size polyester membrane) on six-well tissue culture plates (Costar®), allowing them to be cultured at the air/liquid interface, upon the addition of 1 mL of culture medium. Three

experimental groups were established: control group, femora were cultured with alpha minimum essential medium (α-MEM) supplemented with ascorbic acid (50 µg/mL), amphotericin B (2.5 µg/mL), streptomycin (100 µg/mL) and penicillin (100 units/mL), all Gibco®; mild hyperglycemic group GL12, femora were cultured with the described medium further supplemented with a glucose solution to obtain a final 12 mM glucose concentration; and severe hyperglycemic group GL25, in which femora were cultured with the control culture medium supplemented to obtain a final 25 mM glucose concentration. Such experimental conditions were established in order to represent postprandial glucose levels in DM patients, being 12 mM equivalent to a mild hyperglycemia and 25mM correspondent to severe hyperglycemia [18]. Culture medium for control group presented 5.5 mM of glucose, corresponding to a normoglycemic condition.

The culture plates were maintained at 37ºC, in humidified air with 5% $CO_2$, for eleven days and the culture medium was replaced daily. At day eleven, all specimens were washed twice in phosphate buffered saline (PBS) and frozen or fixed in 4% paraformaldehyde for further analysis.

2.2 Macroscopic assessment

Whole femora were stained with Alcian blue/Alizarin red S histochemical stain, for the visualization of the sulphated glycosaminoglycans-rich tissue in blue, and mineralized tissue in red/purple. Protocol was based in a previous methodology described by Yamazaki et al [38]. In brief, after fixation, femora were rehydrated in 70% alcohol and submerged overnight in an acidic Alcian blue solution - prepared by adding 10 mg of Alcian blue (Sigma®) in a 4:1 ratio of ethanol 95% to acetic acid 99% solution. Then, specimens were progressively rehydrated in solutions of alcohol at 95%, 75%, 40% and 15 %, for two hours in each solution. Following, samples were placed for 48 hours in an Alizarin red S 0.2% solution, prepared in potassium hydroxide (KOH) 0.5%. After macerating for 4 hours in 2% KOH solution, tissue clearing was performed by placing femora, successively, in solutions of 3:1, 1:1 and 1:3 of 0.5% KHO: glycerin, for 8 hours. All specimens were preserved in glycerin.

Stained samples were photographed, and linear measurements were taken using ImageJ software (version 1.51j8) after size calibration. Total linear length and mineralized linear length, the later corresponding to the linear portion stained by Alizarin red, were measured. The ratio between linear mineralized length and total linear length was calculated for all specimens. All measurements are presented in millimeters (mm). The assay was performed in quintuplicates.

2.3 Histological assessment

Histological samples were obtained from all experimental groups. After fixation, samples were embedded in paraffin and 3 µm thickness slices were cut using in a microtome. Sections were deparaffinized, re-hydrated for further staining process using either Alcian blue/Sirius red, Masson´s trichrome or von Kossa histochemical staining techniques, as previously detailed [39]. Alcian blue/Sirius red allows the visualization of the collagenous- (red stain) and Glycosaminoglycans-rich (blue stain) regions. Masson´s trichrome stain further allows the

identification of newly deposited collagenous matrix (blue). Von Kossa stains in dark-brown/black the mineralized tissue. Images were captured with Axiocam 208, Zeiss® coupled to microscope Axiolb 5, Zeiss®. For von Kossa stained samples, mineralized area was measured, using ImageJ software (version 1.51j8), after image segmentation using Otsu algorithm for thresholding [40]. Collagen deposition area was measured for Alcian Blue/Sirius red stained samples, using the same method. The assay was performed in quintuplicates.

2.4 Assessment of protein carbonyl content

Chicken femurs were mechanically homogenized in Tris buffer (0.5 M Tris pH 6.8 with 1% SDS). Total protein amount was determined with the RC/DC assay (BioRad®), accordingly to the manufacturer instructions and protein carbonyl derivatives content was assayed. In brief, a certain volume of bone extracts containing 20 µg of protein was derivatized with dinitrophenylhydrazine by mixing the sample with 1 volume of 12% sodium dodecyl sulfate plus 2 volume of 20 mM dinitrophenylhydrazine, prepared in 10% trifluoroacetic acid. After 30 minutes of dark incubation, 1.5 volume of 2 M Tris/18.3% β-mercaptoethanol was added. The derivatized proteins were diluted in Tris-buffered saline (TBS) to obtain a final concentration of 0.001 µg/µL. A 100 µL volume was slot blotted into a nitrocellulose membrane. Immunodetection of carbonyls was then performed using anti-dinitrophenyl (1:2000; MAB2223, Merck Millipore) as the primary antibody. The bands were visualized with enhanced chemiluminescence (ECL; Advansta, GREISE), according to the supplier's instructions, and images were recorded using a Molecular Imager Gel Doc XR + System (Bio-Rad) and analyzed with ImageLab (version 5.0, Bio-Rad) [41]. The assay was performed in triplicates.

2.5 Microcomputed tomography (µCT) analysis

Whole femora were scanned at 40 KV and 100 µA using a Skyscan 1276 system (Bruker®, Belgium). After, three dimensional reconstructions of all samples were conducted using Nrecon 1.7.4.2 software (Bruker®, Belgium), and a volume of interest (VOI), for further quantitative analysis was determined corresponding to the mid-diaphysis region being defined by measuring 2 mm in length from the femoral midpoint, into the cranial and caudal direction. The following structural parameters: tissue volume ($mm^3$), bone volume/tissue volume ratio (%), tissue surface ($mm^2$), bone surface/bone volume ratio ($mm^{-1}$) and cortical thickness (mm) were calculated, using CTanalyser 1.19.31 software (Brucker®, Belgium). Image thresholding was applied in order to separate mineralized bone from non-mineralized tissue. Three dimensional and two-dimensional images were generated using CTVox software 2.3.2.1 (Bruker®, Belgium). Two dimensional images highlight the mineralized tissue portions. Coronal and axial sections were obtained. The assay was performed in triplicates.

2.6 Gene expression analysis

In order to preserve structural integrity of mRNA, femora from each experimental groups, were instantaneously frozen using liquid nitrogen and total RNA was isolated from DNA and proteins using Trizol® (Invitrogen), according to manufacturer´s instructions. Quality and quantity of total extracted RNA were assessed by UV spectrophotometry (A260/A280) in a NanoDrop® ND-1000 UV-Vis Spectrophotometer. RNA was then processed in order to obtain complementary DNA (cDNA) with a two-step reverse transcription quantitative PCR Kit (NZY tech, BioRad®), according to the manufacturer's instruction. Following, quantitative PCR analysis was conducted in a Bio-Rad iQ5 real-time PCR system (Bio-Rad®) using SYBR Premix Ex Taq kit (Supermix, BioRad®). All optimized primers for specific DNA sequence amplification were acquired from BioRad®. The relative gene expression level was normalized to the GAPDH (Unique Assay ID: qGgaCED0029996) housekeeping gene, based on the $2^{-\Delta\Delta Ct}$ method. Expression of the following genes was evaluated: COL1A2 (Unique Assay ID: qGgaCEd0025365), BMP-2 (Unique Assay ID: qGgaCID0027472), RUNX-2(Unique Assay ID: qGgaCID0019198), SPP-1(Unique Assay ID: qGgaCED0023869), NFkB1(Unique Assay ID: qGgaCID0018536), IL-6 (Unique Assay ID: qGgaCID0027781) and IL-10 (Unique Assay ID: qGgaCED0029223). The assay was performed in sixtuplicates.

2.7 Statistical analysis

Statistical analysis was performed using IBM® SPSS® Statistics (version 26.0, SPSS, USA). Kruskall-wallis nonparametric test was employed and differences between groups were considered to be significant for $p<0.05$.

## 3. Results

3.1 Macroscopic evaluation and morphometric analysis

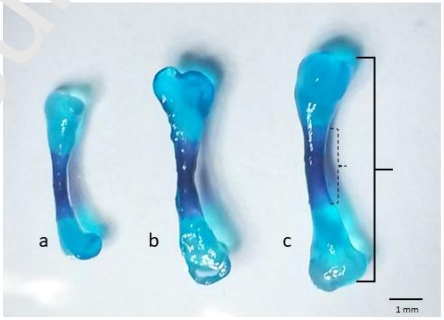


**Fig.1**. Representative macrographs of whole femora macroscopic assessment. a-Control, b-GL12, c-GL25. Scale bar=1mm.

| | Linear measurements (mm) | | | | | |
|---|---|---|---|---|---|---|
| | Total lengh | | Mineralized lengh | | Mineralized Ratio (%) | |
| | Mean | SD | Mean | SD | Mean | SD |
| Control | 9.54 | 0.612 | 3.67 | 0.402 | 38.4 | 2.12 |
| GL 12 | 9.78* | 0.551 | 3.47 | 0.467 | 33.5* | 6.45 |
| GL 25 | 10.26* | 0.377 | 3.22 | 0.418 | 31.3* | 3.02 |

**Table 1**. Morphometric analysis of the whole femora. SD-standard deviation *p<0.05

Macroscopic assessment allowed the identification of mineralized and non-mineralized sections of double stained femora, evidencing a predominant mineralized section at the mid-diaphysis (red stain) and a predominant cartilaginous-rich tissue at the epiphyseal region (blue stain) (Fig.1). No evidences of gross pathological alterations were observed. In addition, morphometric indexes were determined (Table 1). Total linear length was significantly increased in group GL12 and group GL25, as compared to control, suggesting an increased femoral length with the increase of the glucose levels. Regarding to the mineralized section length, no significant differences were found between groups exposed to high glucose concentrations and control. Furthermore, the mineralized ratio was significantly decreased in both GL12 and GL25 groups, as compared to control, revealing that the mineralized section did not follow a proportional increase in relation to total linear length variation.

3.2 Histological/histochemical assessment

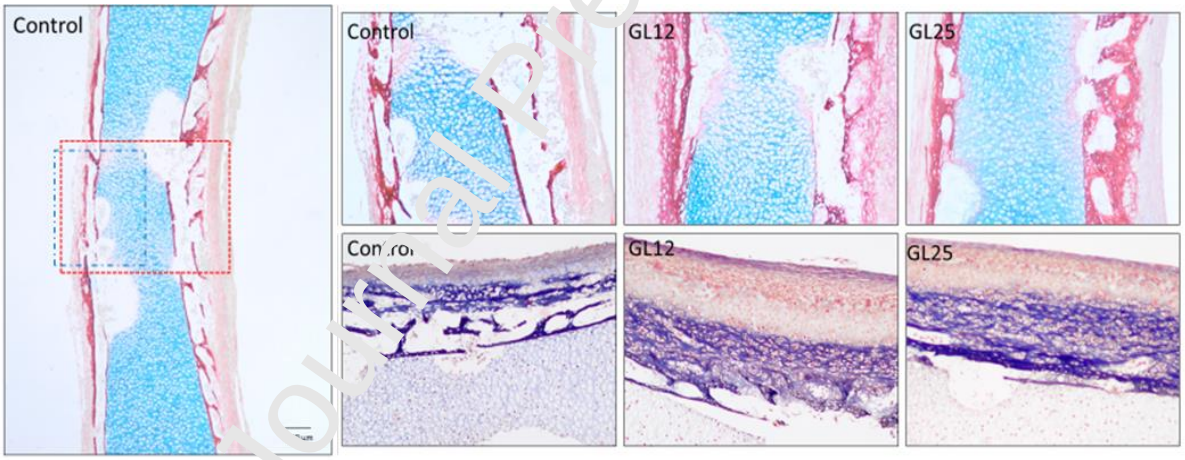


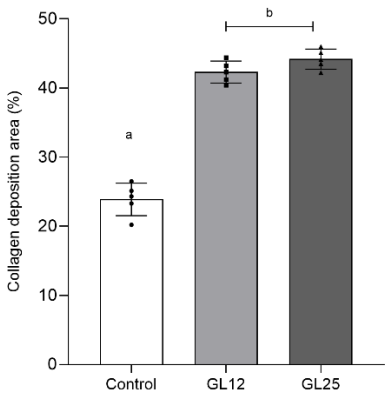

**Fig.2**. Representative micrographs of Alcian blue/Sirius Red and Mason´s Trichrome stained femora (top). Scale bar= 100µm. Quantitative determination of Collagen deposition area (bottom), b is significantly different from a, p<0.05

Close examination of the histological sections of the AB/SR stained femora (Fig. 2, top) allowed to verify a distributed glycosaminoglycan-rich layer in the central portion of the mid-diaphysis (stained in blue), and peripheral collagenous matrix (stained in red), progressively organizing into a trabecular structure. Comparatively, samples of group GL12 and Group GL25 showed an increased collagen-rich structure, evidenced by the increased area of red staining, and further confirmed by collagen deposition area assessment (Fig. 2, bottom). A similar trend was verified in samples stained with Mason´s trichrome (Fig. 2, bottom). Glycosaminoglycan-rich portion showed no evident alterations among groups. It was possible to visualize some areas of condensation in the interfacial region with the collagenous portion, especially evident in samples stained with AB/SR, further evidencing the progressive trabecular organization from the periosteal region towards the lumen, replacing previous areas of cartilage erosion. This process seems to be more advanced in the control group, in which a more defined and well-organized trabecular formation was observed. A similar pattern was attained in Mason´s trichrome stained samples.

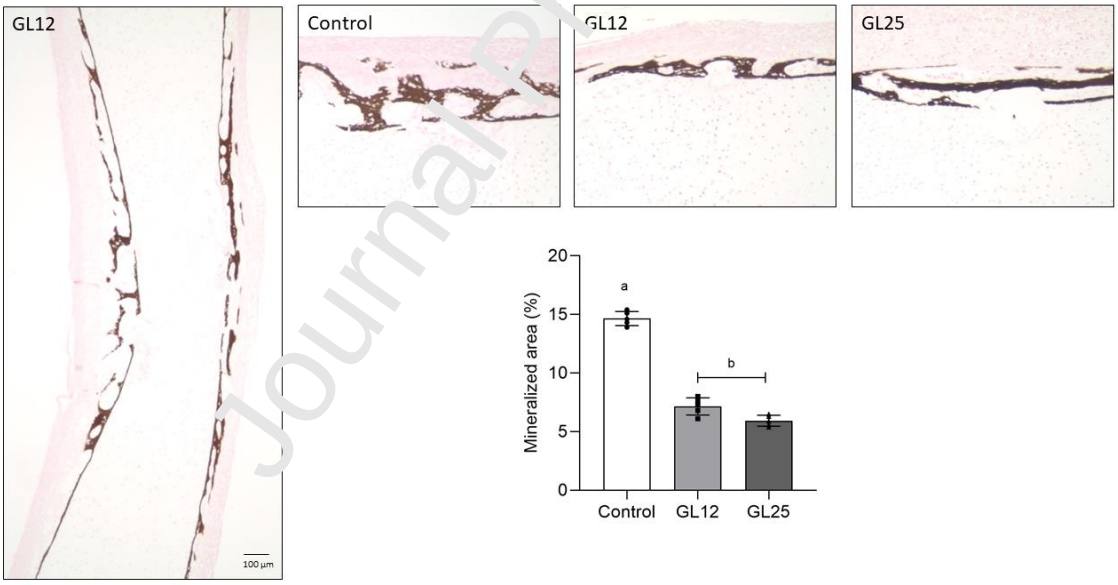


**Fig.3.** Representative micrographs of von Kossa stained femora (top). Scale bar=100µm. Quantitative determination of the mineralized area in histological samples (bottom), b significantly different from a, p<0.05.

Despite the increased collagen deposition in high glucose conditions, the mineralization of the ECM did not follow the same tendency, as it observed in von Kossa-stained samples. The mineral deposits (dark brown/black stain) were sparse in both GL12 and GL25 groups (Fig. 3, top). Images showed a thinner layer of mineralized tissue in samples from group GL12 and group GL25, as compared to control, the later, associated with more mature mineralized

trabecula and increased mineral deposition – as further evidenced by the higher total mineralized area in control, as compared to GL groups (Fig. 3, bottom).

3.3 Assessment of protein carbonyl content

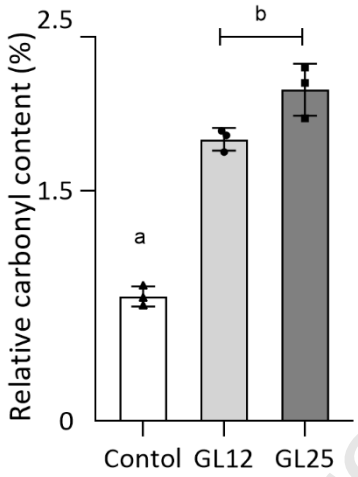


**Fig.4**. Protein carbonyl content results. Graph presents relative amount of protein carbonyl in the experimental groups, b is significantly different from a, $p<0.05$

Protein carbonyl content of the assayed femora was found to be significantly increased in both GL12 and GL25 groups, in comparison with control group (Fig.4). Comparatively, no differences were found between GL12 and GL25.

3.4 Microtomographic analysis

| | Control | | GL12 | | GL25 | |
|---|---|---|---|---|---|---|
| | *Mean* | *SD* | *Mean* | *SD* | *Mean* | *SD* |
| TV ($mm^3$) | 22,36 | 1,63 | 52,85* | 4,77 | 59,41* | 1,10 |
| BV ($mm^3$) | 0,40 | 0,04 | 0,35 | 0,03 | 0,42 | 0,03 |
| BV/TV (%) | 1,79 | 0,11 | 1,39 | 0,37 | 0,69* | 0,03 |
| TS ($mm^2$) | 51,66 | 1,96 | 81,75* | 4,84 | 91,32* | 0,98 |
| BS ($mm^2$) | 17,11 | 1,46 | 15,45 | 1,96 | 18,47 | 2,20 |
| BS/BV ($mm^{-1}$) | 0,77 | 0,02 | 0,57* | 0,06 | 0,31* | 0,04 |
| Ct.TH (mm) | 0.0662 | 0.0023 | 0.0429* | 0.0034 | 0.0384* | 0.0027 |

**Table 2** - Microtomographic histomorphometric analysis of the VOI defined within the mid-diaphysis of cultured femora. TV-total volume, BV/TV-Bone volume/Total Volume, TS-Tissue Surface, BS/BV-Bone Surface/Bone Volume (Bone density), Ct.TH- Cortical Thickness. SD-standard deviation. *$p<0.05$, significantly different from control.

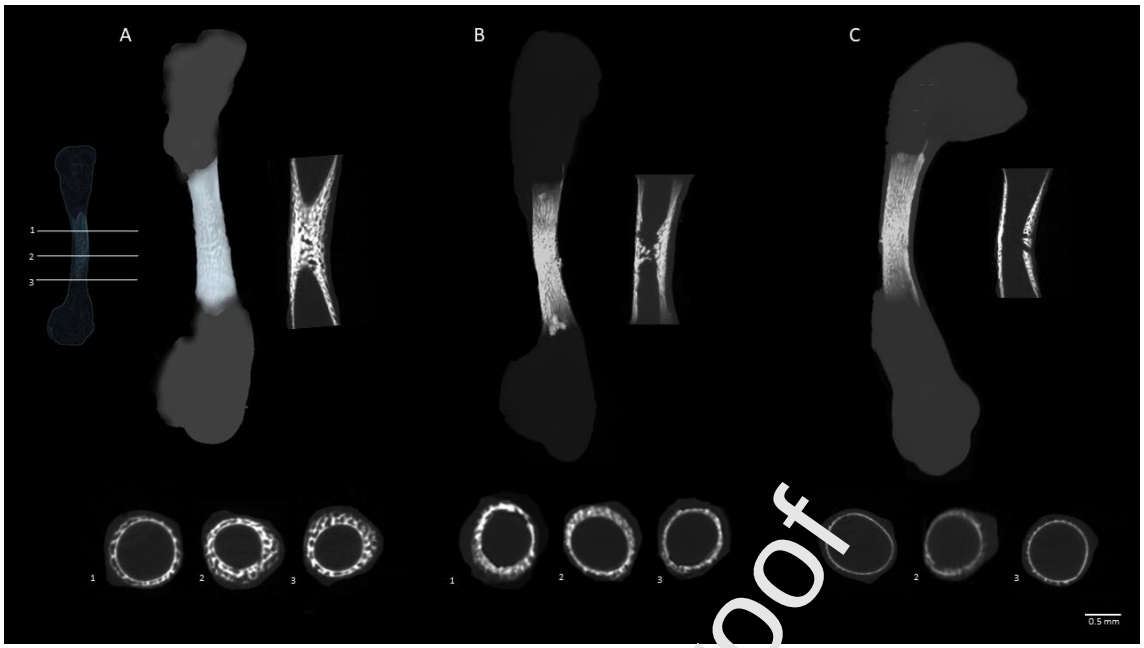


**Fig 5.** Representative microtomographic reconstructions (2D and 3D images) of cultured femora. A-control. B- GL12, C-GL25. 1, 2, 3 represent the cross-sectional level, 1- top; 2- middle; 3 -bottom. Scale bar=0.5mm

Data from µCT shows that within the mid diaphysis region, corresponding to the defined VOI that was submitted to the quantitative analysis, a significant increase in total tissue volume was verified in groups GL12 and GL25, as comparing to femora cultured in basal conditions (control). Further, significant differences were found in BV/TV ratio. Group GL25 presented the lowest BV/TV ratio, with GL12 also presenting significantly reduced values, as compared to control. Contrariwise, TS levels were found to be significantly higher in those femora exposed to high glucose levels, with GL25 attaining the highest values. Lastly, the BS/BV ratio was significantly decreased in high glucose exposed groups, in particular for group GL25, as compared to control.

Images of cross and longitudinal (Fig. 5) sections highlight the clear variation of mineralized surfaces among experimental groups, with an increased mineral content verified within the control at the peripheral regions, evidencing the progressive mineralized trabecular organization. Cortical thickness assessment is further in line with these observations, with a significant higher thickness attained in control, as compared to GL12 and GL25.

3.5 Gene Expression analysis

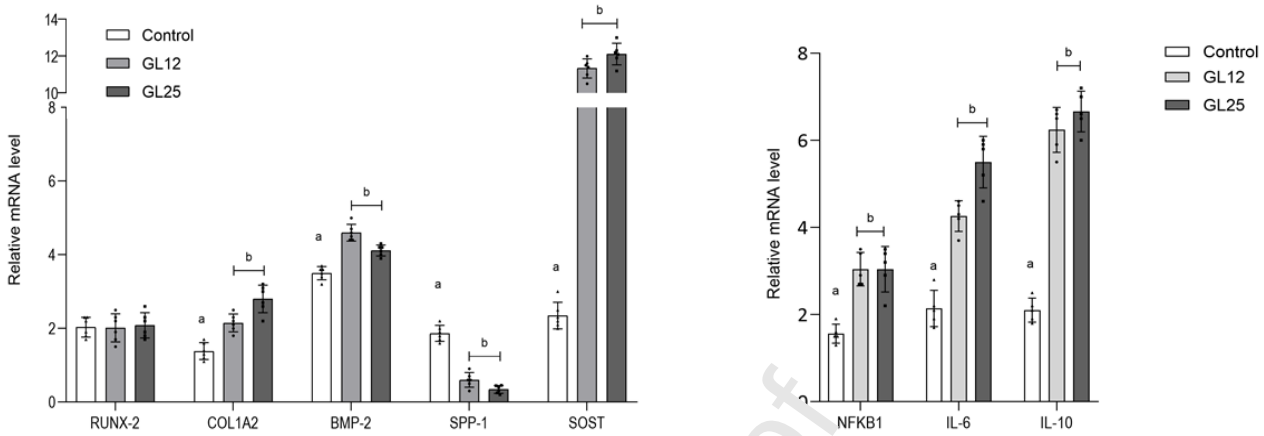


**Fig. 6**. Gene expression analysis of cultured femora, b is significantly different from a, $p<0.05$

Genes associated with early osteogenic activity, COL1A2, RUNX-2 and BMP-2, showed an increased expression in both GL12 and GL25 groups, in comparison with control. SPP1 gene, that encodes osteopontin, a protein associated with late stages of bone mineralization, presented significant decreased levels in both groups exposed to high glucose concentrations (Fig.6, left). On the other hand, SOST gene, that encodes sclerostin, was highly overexpressed in GL12 and GL25 groups. Regarding genes associated with inflammation, i.e. NFKB1, IL-6 and IL-10, an increased relative mRNA level's expression was verified for both GL12 and GL25 groups, as compared to control, attaining the highest expression in the GL25 group (Fig. 6, right).

## 4. Discussion

This study aimed to establish and validate an *ex vivo* model of hyperglycemic-induced bone alterations, through the characterization of the embryonic chicken femur organotypic culture exposed to high glucose concentrations. The experimental conditions for group GL12 and group GL25 were selected in order to replicate the hyperglycemic condition of DM patients, being representative of mild glucose levels (12mM), equivalent of 216 mg/dL postprandial blood glucose concentration, and severe glucose level (25 mM), equivalent to approximately 432 mg/dl postprandial blood glucose concentration [18, 26]. Likewise, culture conditions of the control group mimic a normoglycemic condition that corresponds to around 5.5 mM of glucose, that is equivalent to 99 mg/dL postprandial glucose concentration. This concentration is, by default, the glucose concentration present in the culture medium.

In brief, major structural, histological and biological alterations were identified in femora cultured in high glucose conditions. Macroscopic evaluation showed that samples from GL12 and GL25 groups presented an increased length, being suggestive of an increased metabolic activity of bone cells and enhanced cell proliferation. *In vitro* studies report a similar trend on the cell proliferative potential as a result of the hyperglycemic environment. Al-Qarakhli et al reported that bone marrow MSCs display an increase proliferation when cultured in high glucose-supplemented media [20]. Also, Freude et al reported that human osteoblasts present increased proliferation *in vitro*, when exposed to high levels of glucose [42]. The increased cell proliferation seems to be the result of a positive energetic output due to the availability of glucose [20, 42]. Osteoblasts rely mainly on glycolysis to generate the energy required to cell metabolism, so increased glucose availability is expected to upregulate metabolic activity [43].

Histological analysis further support these observations since it is clear the increasing tissue formation and collagen deposition in samples from both GL12 and GL25 groups, being evident with either AB/SR or Masonʼs trichrome histochemical stains. Cunha et al described, in their in *vitro* study, that osteoblasts cultured in very high glucose conditions had remarkable increased collagen production, when compared with osteoblast cultured in basal conditions [44]. Similar observations were made by Zayzafoon et al [45] in their *in vitro* study, describing that acute exposure to high levels of glucose increased the expression of type I collagen mRNA by osteoblasts. In our study, gene expression analysis further supported these observations, since COL1A2 gene showed an increased expression in groups GL12 and GL25, pointing to an increased metabolic activity of osteoblasts along with an enhanced collagen transcription and synthesis. Although it remains elusive how hyperglycemic condition enhances collagen production, it seems to relate to the upsurge of the osmotic pressure mediated by the by the glucose content within the microenvironment. Osmotic pressure may induce volumetric changes in the cellular compartments that triggers an adaptive response, leading to an active gene expression and metabolic alterations, as described in previous *in vitro* studies [19, 44].

Collagen deposition in ECM is a key process, essential for bone tissue formation and maturation [22]. However, the results of the protein carbonyl content assay, which is a major indicator of protein damage as result of increasing oxidative stress levels, indicated that

collagen structure may present abnormalities as a result of the glucose exposure [46], since the high glucose concentration-exposed groups presented the highest content of carbonyl. It is reported that oxidative stress is a consequence of hyperglycemia in DM patients [13, 23]. Moreover, high levels of oxidative stress are highly related with the formation of AGEs, as result of non-enzymatic mediated glycation of amino terminal groups of the protein chains, which is reported as one of the major alterations of collagen structure in the context of the disease [47-50]. Kitamura et al demonstrated using a zebrafish model that hyperglycemic condition severely altered the collagen protein structure due to AGEs accumulation, even upon a short period of exposure [51]. Therefore, attained results further converge to justify that despite the attained enhancement of the collagen-related gene expression and protein synthesis, a damaged protein structure was attained upon the exposure to high glucose conditions [33, 52].

Of additional relevance, and despite the increased expression of early osteogenic-related genes, the mineralization process seems to be severely impaired by the exposure to high glucose levels. SPP-1 gene expression is decreased under the influence of high glucose levels. SPP-1 gene encodes osteopontin, which is a protein associated with late stages of osteoblastic differentiation, being crucial to mediate ECM mineralization [53, 54]. In accordance, von Kossa staining evidences the decreased amount of mineralized tissue present in both hyperglycemic groups, whether the impairment seems to be more evident in the GL25 group. Microtomographic analysis that allows the morphometric assessment of the mineralized tissue, further confirms that GL12 and GL25 groups had a decreased mineralized tissue amount, given the reduced BV/TV and BS/BV ratios, as well as a decreased cortical thickness. Such observations are supported by previous studies. Cunha et al demonstrated that mineralization process is impaired in osteoblastic cells by high levels of glucose, despite the elevated collagen deposition [44], in line with the presently attained data. Similar findings were described within *in vivo* studies with rodents. Mohsin et al [55], and Silva et al [56] reported, in their works, that bone structure is affected in rats with DM, with decrease bone mechanical proprieties as result of decreased matrix mineralization. Limirio et al also reported that bone biomechanical properties in diabetic rats are compromised due to the lack of proper collagen maturation, leading to loss of bone mineral content [10]. Mohsin at al referred that bone quality alterations in diabetic rats are even associated with the early stages of DM [55], being consistent with present study that establishes that the exposure to high glucose concentrations induces alteration on bone metabolism/development, even upon a short-term exposure.

Another interest finding of the present research was that the SOST gene, that encodes sclerostin, was highly overexpressed in GL12 and GL25 groups. Since SOST is also associated with the late stages of bone cell differentiation, its increased expression levels may seem contradictory, considering the supporting data of osteoblastic differentiation impairment. In fact, sclerostin downregulates the Wnt/β-catenin signaling pathway that plays a crucial role for maintenance of bone metabolism, being overexpressed under certain pathological conditions, including DM [57-59]. Several studies, performed *in vivo* and *in vitro*, demonstrated that increasing expression of SOST results in the suppression of bone formation with subsequent

loss of bone mass and bone volume. Also, elevated sclerostin levels are found among DM patients [8, 59]. Pacicca et al suggested that SOST overexpression is the direct result of glucose effect on bone cells, either *in vitro* or *in vivo* [60], as verified within our ex vivo system.

Of additional relevance, it is described that SOST overexpression is associated with increasing levels of pro-inflammatory cytokines. Present results show that IL-6 and IL-10 are overexpressed in hyperglycemic groups, along with NFKB1 gene, which regulates the transcription of multiple inflammation-related mediators [61]. In addition, pro-inflammatory mediators are also described to be associated with increasing level of oxidative stress, that may lead to protein damage, as it is suggested by carbonyl content assay results, leading to possible impairment of collagen structure that consequently hinders ECM mineralization process. Previous studies demonstrate that AGEs formation with subsequent increasing levels of oxygen reactive species trigger an inflammatory response by increasing NFKB gene transcription [48, 49], being coherent with the present study findings. Moreover, present results demonstrate that an enhanced pro-inflammatory response to high glucose conditions is the result of a local effect on bone cells, independent from a systemic inflammatory regulation.

To the best of authors' knowledge, there is no other study evaluating the effects of high glucose concentrations in an *ex vivo* model of the bone tissue metabolism/development. The present findings highlight the model functionality and responsiveness to distinct glucose levels, showcasing its integrative capability to display the acknowledged hyperglycemia-mediated alterations on bone tissue development that affect cell proliferation and metabolic activity, alter gene and protein expression levels, impair osteogenesis, enhance inflammatory priming, globally converging to an altered tissue morphological and functional arrangement, with impaired mineralization. Whether the attained findings may be representative within developing organisms, further studies may be required to establish the translatability of the present data as representative of hyperglycemia-induced alterations on the adult skeleton.

## 5. Conclusion

The organotypic embryonic chick femur exposed to high glucose levels may be regarded as a new and valuable model of the bone tissue response to hyperglycemia-induced alterations. The *ex vivo* model displayed an integrative response to high glucose concentrations, coherent with the acknowledged hyperglycemia-induced alterations of the bone tissue in diabetic conditions. The model allows the assessment of cellular functionality-related parameters, as well as of tissue-related alterations, without the interference of systemic factors and/or regulatory systems, outreaching the attained limitations of current *in vitro* and *in vivo* models.

## Funding

Authors acknowledge Fundação para a Ciência e Tecnologia (FCT) for the financial support under the project UIDB/50006/2020.

## Author Contribution

Rita Araújo: Conceptualization, Methodology, Investigation, Writing – original draft preparation. Victor Martin: Investigation, Formal analysis. Rita Ferreira: Investigation, Resources. Maria Helena Fernandes: Funding acquisition, Validation, Writing -reviewing and editing. Pedro de Sousa Gomes: Conceptualization, Data curation, Methodology, Project Administration, Writing – reviewing and editing.

**Declaration of competing interests**

The authors declare no competing interests.

**Acknowledgements**

The authors acknowledge the support of the i3S Scientific Platform Bioimaging, member of the PPBI (PPBI-POCI-01-0145-FEDER-022122), as well as HEMS - Histology and Electron Microscopy Department.

**6. References**

1. Cole, J.B. and J.C. Florez, *Genetics of diabetes mellitus and diabetes complications.* Nat Rev Nephrol, 2020. 16(7): p. 377-390.
2. Olokoba, A.B., O.A. Obateru, and L.B. Olokoba, *Type 2 diabetes mellitus: a review of current trends.* Oman Med J, 2012. 27(4): p. 269-73.
3. Raisingani, M., et al., *Skeletal growth and bone mineral acquisition in type 1 diabetic children; abnormalities of the GH/IGF-1 axis.* Growth Hormone & IGF Research, 2017. 34: p. 13-21.
4. Tuomilehto, J., et al., *Prevention of type 2 diabetes mellitus by changes in lifestyle among subjects with impaired glucose tolerance.* N Engl J Med, 2001. 344(18): p. 1343-50.
5. Viguet-Carrin, S., P. Garnero, and P.D. Delmas, *The role of collagen in bone strength.* Osteoporos Int, 2006. 17(3): p. 319-36.
6. de Paula, F.J.A., M.C. Horowitz, and C.J. Rosen, *Novel insights into the relationship between diabetes and osteoporosis.* Diabetes/Metabolism Research and Reviews, 2010. 26(8): p. 622-630.
7. Napoli, N., et al., *The Alliance of Mesenchymal Stem Cells, Bone, and Diabetes.* International Journal of Endocrinology, 2014. 2014: p. 690783.
8. Kalaitzoglou, E., et al., *Effects of Type 1 Diabetes on Osteoblasts, Osteocytes, and Osteoclasts.* Curr Osteoporos Rep, 2016. 14(6): p. 310-319.
9. Wang, A., et al., *Hyperglycemia diverts dividing osteoblastic precursor cells to an adipogenic pathway and induces synthesis of a hyaluronan matrix that is adhesive for monocytes.* J Biol Chem, 2014. 289(16): p. 11410-11420.
10. Limirio, P.H.J.O., et al., *Influence of hyperbaric oxygen on biomechanics and structural bone matrix in type 1 diabetes mellitus rats.* PLOS ONE, 2018. 13(2): p. e0191694.
11. Chen, S., et al., *Differential effects of type 1 diabetes mellitus and subsequent osteoblastic β-catenin activation on trabecular and cortical bone in a mouse model.* Experimental & Molecular Medicine, 2018. 50(12): p. 1-14.
12. Hunt, H.B., et al., *Bone Tissue Collagen Maturity and Mineral Content Increase With Sustained Hyperglycemia in the KK-Ay Murine Model of Type 2 Diabetes.* J Bone Miner Res, 2018. 33(5): p. 921-929.
13. Kanazawa, I. and T. Sugimoto, *Diabetes Mellitus-induced Bone Fragility.* Intern Med, 2018. 57(19): p. 2773-2785.

14. Jackuliak, P. and J. Payer, *Osteoporosis, Fractures, and Diabetes.* International Journal of Endocrinology, 2014. 2014: p. 820615.
15. Lekkala, S., et al., *Effects of Diabetes on Bone Material Properties.* Curr Osteoporos Rep, 2019. 17(6): p. 455-464.
16. Lecka-Czernik, B., *Diabetes, bone and glucose-lowering agents: basic biology.* Diabetologia, 2017. 60(7): p. 1163-1169.
17. Costantini, S. and C. Conte, *Bone health in diabetes and prediabetes.* World journal of diabetes, 2019. 10(8): p. 421-445.
18. García-Hernández, A., et al., *High Glucose concentrations alter the biomineralization process in human osteoblastic cells.* Bone, 2012. 50(1): p. 276-88.
19. Botolin, S. and L.R. McCabe, *Chronic hyperglycemia modulates osteoblast gene expression through osmotic and non-osmotic pathways.* J Cell Biochem, 2006. 99(2): p. 411-24.
20. Al-Qarakhli, A.M.A., et al., *Effects of high glucose conditions on the expansion and differentiation capabilities of mesenchymal stromal cells derived from rat endosteal niche.* BMC Molecular and Cell Biology, 2019. 20(1): p. 51.
21. Wang, J.F., et al., *Bone Morphogenetic Protein-6 Attenuates Type 1 Diabetes Mellitus-Associated Bone Loss.* Stem Cells Transl Med, 2019. 8(6): p. 522-534.
22. Shahi, M., A. Peymani, and M. Sahmani, *Regulation of Bone Metabolism.* Rep Biochem Mol Biol, 2017. 5(2): p. 73-82.
23. Stefano, G.B., S. Challenger, and R.M. Kream, *Hyperglycemia-associated alterations in cellular signaling and dysregulated mitochondrial bioenergetics in human metabolic disorders.* Eur J Nutr, 2016. 55(8): p. 2339-2345.
24. Blair, H.C., et al., *Osteoblast Differentiation and Bone Matrix Formation In Vivo and In Vitro.* Tissue Eng Part B Rev, 2017. 23(3): p. 268-280.
25. Gopalakrishnan, V., et al., *Effects of glucose and its modulation by insulin and estradiol on BMSC differentiation into osteoblastic lineages.* Biochem Cell Biol, 2006. 84(1): p. 93-101.
26. Filion, T.M., et al., *Impaired osteogenesis of T1DM bone marrow-derived stromal cells and periosteum-derived cells and their differential in-vitro responses to growth factor rescue.* Stem Cell Res Ther, 2017. 8(1): p. 65.
27. Rinker, T.E., et al., *Interactions between mesenchymal stem cells, adipocytes, and osteoblasts in a 3D tri-culture model of hyperglycemic conditions in the bone marrow microenvironment.* Integr Biol (Camb), 2014. 6(3): p. 324-37.
28. Moseley, K.F., M.E. Doyle, and S.M. Jan De Beur, *Diabetic serum from older women increases adipogenic differentiation in mesenchymal stem cells.* Endocr Res, 2018. 43(3): p. 155-165.
29. Cramer, E.E.A., K. Ito, and S. Hofmann, *Ex vivo Bone Models and Their Potential in Preclinical Evaluation.* Current Osteoporosis Reports, 2021. 19(1): p. 75-87.
30. Papadimitriou, K., et al., *Ex Vivo Models Simulating the Bone Marrow Environment and Predicting Response to Therapy in Multiple Myeloma.* Cancers, 2020. 12(8): p. 2006.
31. Marin, C., et al., *The Impact of Type 2 Diabetes on Bone Fracture Healing.* Frontiers in Endocrinology, 2018. 9(6).
32. Cipriani, C., et al., *The Interplay Between Bone and Glucose Metabolism.* Frontiers in Endocrinology, 2020. 11(122).
33. Al-Hariri, M., *Sweet Bones: The Pathogenesis of Bone Alteration in Diabetes.* Journal of Diabetes Research, 2016. 2016: p. 6969040.
34. Smith, E., J. Kanczler, and R. Oreffo, *A new take on an old story: Chick limb organ culture for skeletal niche development and regenerative medicine evaluation.* European cells & materials, 2013. 26: p. 91-106.

35. Smith, E.L., et al., *Evaluation of skeletal tissue repair, Part 1: Assessment of novel growth-factor-releasing hydrogels in an ex vivo chick femur defect model.* Acta Biomaterialia, 2014. 10(10): p. 4186-4196.
36. Smith, E.L., et al., *Evaluation of skeletal tissue repair, Part 2: Enhancement of skeletal tissue repair through dual-growth-factor-releasing hydrogels within an ex vivo chick femur defect model.* Acta Biomaterialia, 2014. 10(10): p. 4197-4205.
37. Barros, J.A.R., et al., *Encapsulated bacteriophages in alginate-nanohydroxyapatite hydrogel as a novel delivery system to prevent orthopedic implant-associated infections.* Nanomedicine: Nanotechnology, Biology and Medicine, 2020. 24: p. 102145.
38. Yamazaki, Y., et al., *Whole-mount bone and cartilage staining of chick embryos with minimal decalcification.* Biotechnic & Histochemistry, 2011. 86(5): p. 351-358.
39. Gomes, P.S., et al., *The Osteogenic Assessment of Mineral Trioxide Aggregate–based Endodontic Sealers in an Organotypic Ex Vivo Bone Development Model.* Journal of Endodontics, 2021. 47(9): p. 1461-1466.
40. Otsu, N., *A Threshold Selection Method from Gray-Level Histograms.* IEEE Transactions on Systems, Man, and Cybernetics, 1979. 9(1): p. 62-66.
41. Padrão, A.I., et al., *OXPHOS susceptibility to oxidative modifications: the role of heart mitochondrial subcellular location.* Biochimica et biophysica acta, 2011. 1807 9: p. 1106-13.
42. Freude, T., et al., *Hyperinsulinemia reduces osteoblast activity in vitro via upregulation of TGF-β.* Journal of Molecular Medicine, 2012. 90(11): p. 1257-1266.
43. Yang, J., H. Ueharu, and Y. Mishina, *Energy metabolism: A newly emerging target of BMP signaling in bone homeostasis.* Bone, 2020. 138: p. 115467-115467.
44. Cunha, J.S., et al., *Effects of high glucose and high insulin concentrations on osteoblast function in vitro.* Cell and Tissue Research, 2014. 358(1): p. 249-256.
45. Zayzafoon, M., et al., *Extracellular glucose influences osteoblast differentiation and c-Jun expression.* J Cell Biochem, 2000. 79(2): p. 301-10.
46. Burcham, P.C., *Modified protein carbonyl assay detects oxidised membrane proteins: A new tool for assessing drug- and chemically-induced oxidative cell injury.* Journal of Pharmacological and Toxicological Methods, 2007. 56(1): p. 18-22.
47. Yamamoto, M. and T. Sugimoto, *Advanced GLycation End Products, Diabetes, and Bone Strength.* Curr Osteoporos Rep, 2016. 14(6): p. 320-326.
48. Rains, J.L. and S.K. Jain, *Oxidative stress, insulin signaling, and diabetes.* Free Radic Biol Med, 2011. 50(5): p. 567-75.
49. Nowotny, K., et al., *Advanced Glycation end products and oxidative stress in type 2 diabetes mellitus.* Biomolecules, 2015. 5(1): p. 194-222.
50. Newsholme, P., et al., *Molecular mechanisms of ROS production and oxidative stress in diabetes.* Biochem J, 2016. 473(24): p. 4527-4550.
51. Kitamura, K.-i., et al., *Effects of hyperglycemia on bone metabolism and bone matrix in goldfish scales.* Comparative Biochemistry and Physiology Part A: Molecular & Integrative Physiology, 2017. 203: p. 152-158.
52. Arseni, L., A. Lombardi, and D. Orioli, *From Structure to Phenotype: Impact of Collagen Alterations on Human Health.* International Journal of Molecular Sciences, 2018. 19(5): p. 1407.
53. De Fusco, C., et al., *Osteopontin: Relation between Adipose Tissue and Bone Homeostasis.* Stem Cells International, 2017. 2017: p. 4045238.
54. Subraman, V., et al., *OPN -Revisited.* J Clin Diagn Res, 2015. 9(6): p. Ze10-3.
55. Mohsin, S., et al., *In vivo Labeling of Bone Microdamage in an Animal Model of Type 1 Diabetes Mellitus.* Scientific Reports, 2019. 9(1): p. 16994.

56. Silva, M.J., et al., *Type 1 diabetes in young rats leads to progressive trabecular bone loss, cessation of cortical bone growth, and diminished whole bone strength and fatigue life.* J Bone Miner Res, 2009. 24(9): p. 1618-27.
57. Delgado-Calle, J., A.Y. Sato, and T. Bellido, *Role and mechanism of action of sclerostin in bone.* Bone, 2017. 96: p. 29-37.
58. Galea, G.L., L.E. Lanyon, and J.S. Price, *Sclerostin's role in bone's adaptive response to mechanical loading.* Bone, 2017. 96: p. 38-44.
59. Kang, J., et al., *Hyperglycemia increases the expression levels of sclerostin in a reactive oxygen species- and tumor necrosis factor-alpha-dependent manner.* J Periodontal Implant Sci, 2015. 45(3): p. 101-110.
60. Pacicca, D.M., et al., *Elevated Glucose acts directly on osteocytes to increase sclerostin expression in diabetes.* Sci Rep, 2019. 9(1): p. 17353.
61. Clem, K.W. and Y.T. Ip, *Nuclear Factor-kappa B*, in *Gene Expression and Regulation*, J. Ma, Editor. 2006, Springer New York: New York, NY. p. 321-327.

# CRediT roles

Rita Araújo: Formal analysis, Investigation, Methodology, Writing - original draft

Victor Martin: Data curation, Formal analysis

Rita Ferreira: Methodology

Maria Helena Fernandes: Project administration, Writing - review & editing

Pedro Sousa Gomes: Supervision, Conceptualization, Writing - review & editing

Highlights

- An ex vivo model of the bone tissue response to hyperglycemia was established
- Morphometric, microstructural and histomorphometric alterations were reported
- An altered osteogenic and inflammatory gene expression was identified
- This model is a representative organotypic system for hyperglycemia-related research